

Avoiding escapes in open dynamical systems using phase control

Jesús M. Seoane,^{1,*} Samuel Zambrano,^{1,†} Stefano Euzzor,² R. Meucci,² F. T. Arcchi,^{2,3} and Miguel A.F. Sanjuán¹

¹*Nonlinear Dynamics and Chaos Group, Departamento de Física, Universidad Rey Juan Carlos, Tulipán s/n, 28933 Móstoles, Madrid, Spain*

²*CNR-Istituto Nazionale di Ottica Applicata, Largo E. Fermi, 6 50125 Firenze, Italy*

³*Department of Physics, Università di Firenze, Firenze, Italy*

(Received 13 July 2007; revised manuscript received 30 May 2008; published 8 July 2008)

In this paper we study how to avoid escapes in open dynamical systems in the presence of dissipation and forcing, as it occurs in realistic physical situations. We use as a prototype model the Helmholtz oscillator, which is the simplest nonlinear oscillator with escapes. For some parameter values, this oscillator presents a critical value of the forcing for which all particles escape from its single well. By using the phase control technique, weakly changing the shape of the potential via a periodic perturbation of suitable phase ϕ , we avoid the escapes in different regions of the phase space. We provide numerical evidence, heuristic arguments, and an experimental implementation in an electronic circuit of this phenomenon. Finally, we expect that this method might be useful for avoiding escapes in more complicated physical situations.

DOI: [10.1103/PhysRevE.78.016205](https://doi.org/10.1103/PhysRevE.78.016205)

PACS number(s): 05.45.Ac, 05.45.Df, 05.45.Pq

I. INTRODUCTION

Open dynamical systems are typical in nature. In an open dynamical system, there is a region in phase space where nearly all the trajectories diverge asymptotically to infinity. They have attracted a great deal of attention in the context of transient chaos [1] and, particularly, in chaotic scattering problems [2–5], among others. The widespread nature of this type of dynamical systems suggests that there are situations in which we might be interested in avoiding these divergences to infinity, that we refer to as escapes. In order to define what is an escape we can imagine the following scenario. We suppose that a particle is under the influence of some potential or massive object. Under this situation, we say that a dynamical system has an escape whenever this particle crosses a certain boundary and never comes back [6].

Since the pioneering work on controlling chaos due to Ott, Grebogi, and Yorke (OGY) [7], different control schemes have been proposed that allow one to obtain a desired response from a dynamical system by applying some small but accurately chosen perturbations. In this context, some techniques that allow avoiding escapes in open dynamical systems presenting transient chaos have been proposed, with applications to many different situations in physics and engineering (see Ref. [8], and references therein).

The methods stated to control chaos can be classified in feedback and nonfeedback methods [9], depending on how they interact with the system. Feedback methods of chaos control, as the celebrated OGY [7], stabilize one of the unstable orbits that lie in the chaotic attractor by using small state-dependent perturbations into the system. However, in experimental implementations, the fast response that these methods require cannot usually be provided. For these situations, nonfeedback methods are more useful. Nonfeedback methods have been mainly used to suppress chaos in periodically

driven dynamical systems. Among them a broad class is represented by the classical nonlinear oscillators whose general equation reads

$$\ddot{x} + \mu\dot{x} + \frac{dV}{dx} = F \cos(\omega t), \quad (1)$$

where μ is the damping coefficient, $V(x)$ is the potential function responsible for the restoring force acting on the system, and $F \cos(\omega t)$ is an external periodic forcing. Obviously, depending on the potential $V(x)$ we have different kinds of oscillators.

The main idea of these nonfeedback methods is to apply a harmonic perturbation either to some of the parameters of the system or as an additional forcing, being its effectiveness shown numerically and experimentally in different works [10,11]. In Ref. [11], it was observed that the phase difference ϕ between the periodic forcing and the perturbation had certain influence on the dynamical behavior of the system. Furthermore, in Ref. [12], the authors have shown that ϕ plays a crucial role on the global dynamics of the system. This control technique, where ϕ acts as a fixed control parameter, is called “phase control of chaos” and it has been used in Refs. [13,14].

Our aim in this paper is to show that the phase control method can be applied to prevent escapes in open dynamical systems, as well. We use the Helmholtz oscillator as a paradigm of this type of systems, and we show here that the phase control method is also a powerful tool to control and avoid escapes. The authors focused on the transient chaos and its lifetime using practical Lyapunov exponents. Other works on the study of both escapes in a potential barrier and the estimation of the average escape times in a driven model in a noisy environment are described in Refs. [15,16]. In Ref. [15] the authors focused on the influence of noise on the escapes in potential barriers studying both instantaneous and average escape times by using path-integral methods. Finally, Ref. [16] is oriented in the analysis of the distribution of escape times out of a metastable well for a stochastic

*jesus.seoane@urjc.es

†samuel.zambrano@urjc.es

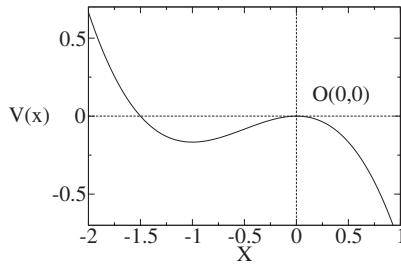


FIG. 1. Plot of the cubic potential $V(x) = -\frac{x^2}{2} - \frac{x^3}{3}$.

model driven by a large-amplitude sinusoidal time-dependent field. These last two works are related with our paper since they study escapes from a potential barrier but they are not in the control framework.

This paper is organized as follows. In Sec. II we present the Helmholtz oscillator and we give a description of our implementation of the phase control. Section III presents numerical simulations showing that the phase control can avoid escapes in many different situations. Some heuristic arguments explaining how this method can tame the escapes in this system are given in Sec. IV. Finally, we give experimental evidence of the validity and robustness of this method by implementing it on an electronic circuit, as described in Sec. V. Conclusions and discussions of the results are presented in Sec. VI.

II. MODEL DESCRIPTION

A paradigmatic example of a dynamical system with escapes is the Helmholtz oscillator. This is the simplest way to model physical phenomena that present the ability to escape from a potential well. This nonlinear oscillator describes the motion of a unit mass particle in a cubic potential $V(x) = ax^2/2 + bx^3/3$, which eventually can be externally perturbed by a sinusoidal driving. By adding a linear dissipative force, the equation of motion is

$$\ddot{x} + \mu\dot{x} + ax + bx^2 = F \cos(\omega t), \quad (2)$$

where μ represents the damping coefficient, F the forcing amplitude, ω the forcing frequency, and a and b determine the shape of the potential.

We fix the parameters all throughout this paper to be $\mu = 0.1$, $\omega = 1$, and $a = b = -1$, for which the potential reads

$$V(x) = -\frac{x^2}{2} - \frac{x^3}{3}. \quad (3)$$

This potential has a maximum at $x = 0$ and a minimum at $x = -1$ as shown in Fig. 1. For this choice of parameter values the equation of motion is

$$\ddot{x} + 0.1\dot{x} - x - x^2 = F \cos t. \quad (4)$$

Note that the only free parameter is the forcing amplitude F . This simple system has been studied previously in several works. For instance, a thorough analysis about its dynamics can be found in Ref. [19], and work on the integrability and symmetry breaking of this oscillator is presented in Refs. [20,21].

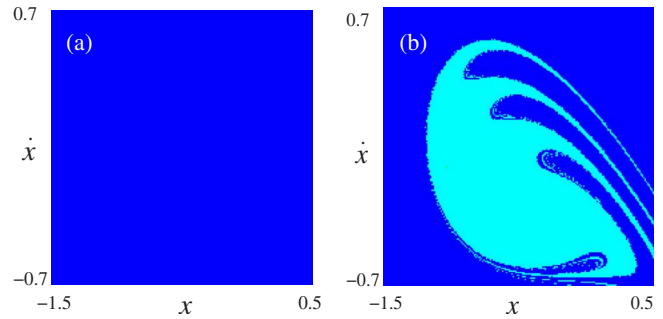


FIG. 2. (Color online) (a) Basin of attraction of the Helmholtz oscillator $\ddot{x} + 0.1\dot{x} - x - x^2 = 0.21 \cos t$. We denote blue (black) dots as the set of points that escape from the potential well, and cyan (pale gray) dots as the points that fall into the attractor(s). Note that in this picture all initial conditions escape after some period of time. (b) Basin of attraction of the Helmholtz oscillator $\ddot{x} + 0.1\dot{x} - x - x^2 = 0.12 \cos t$. Here the basins in phase space have a fractal structure where cyan points (pale gray) denote the set of points falling into the attractors [23].

This system presents different behaviors depending on the value of the forcing amplitude F . For example, we can see a plot of the basins of attraction for this system for $F = 0.12$ and $F = 0.21$ in Fig. 2. In Fig. 2(b), which corresponds to the basin of attraction for $F = 0.12$, a bounded attractor [inside the cyan (pale gray) region] coexists with escaping orbits [blue (cyan) dots]. The attractor corresponds to a bounded orbit, which can be seen in Fig. 3. However, if we take an initial condition from any point of the basin of attraction of Fig. 2(a), the resulting trajectory diverges to infinity, or it simply escapes. In general, a trajectory escapes from the well when it crosses with positive velocity the maximum of the potential situated at $x = 0$ (see Fig. 1) and never comes back. The time spent by a certain particle which is situated inside the well until crossing the maximum of the potential is called the escape time T .

The basins of attraction for $F = 0.21$, shown in Fig. 2(a), show that for this value of the forcing all trajectories escape. This is the situation that we want to control, and this is the value of the forcing F that we consider in the remainder of this paper. Our main goal here is to avoid escapes for the

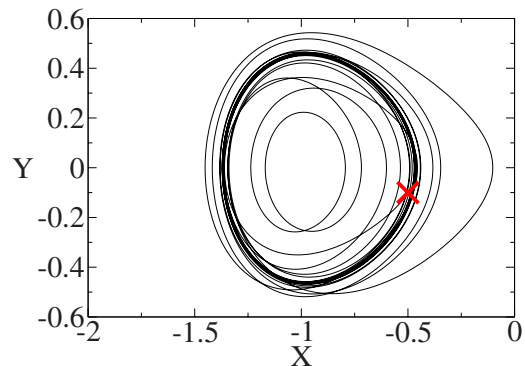


FIG. 3. (Color online) This figure shows the phase space trajectory of the Helmholtz oscillator $\ddot{x} + 0.1\dot{x} - x - x^2 = 0.12 \cos t$ with an initial condition at the point $(x_0, \dot{x}_0) = (-0.5, -0.1)$, indicated by a cross. The dark color indicates the attractor. (Notice that $y = \dot{x}$.)

largest number of initial conditions using the phase control method.

There are different ways to implement the phase control: either by adding a second periodic forcing [12] or by perturbing harmonically one of the parameters of the system [13]. After this, we just need to vary the phase ϕ in search of the desired dynamical behavior. Now we introduce some arguments in order to understand better what is the best strategy in our case.

Suppose we have particles oscillating inside a potential well and an external forcing is acting. These particles can remain inside the well or escape from it depending on the amplitude forcing. A suitable way to modify the dynamical behavior of the particles inside the well is by modifying the shape of the potential well. Following this reasoning, we introduce, as in Ref. [13], a parametric perturbation in the quadratic term of the equation of motion

$$\ddot{x} + 0.1\dot{x} - x - [1 + \epsilon \cos(t + \phi)]x^2 = F \cos(\omega t), \quad (5)$$

where ϵ is the modulation amplitude and ϕ is the phase difference with the forcing that we simply call the phase. Note that we are using for the parametric perturbation a resonant frequency with the forcing amplitude, which is a common assumption for this type of nonfeedback control methods. The effects of a frequency mismatch, which might appear in some experimental situations, will be discussed in Sec. V.

The modulation term $[1 + \epsilon \cos(t + \phi)]$ can be interpreted as a modulation of the potential of the system, which can be rewritten as $V_{\text{pert}}(x, t) = -x^2/2 - [1 + \epsilon \cos(t + \phi)]x^3/3$. In fact, this perturbed potential has a maximum on $x=0$, for which $V_{\text{pert}}(0, t) = 0$. The potential is also zero for $x_{\text{zero}}(t) = -\frac{3}{2[1 + \epsilon \cos(t + \phi)]}$, so the width of the potential is $|\Delta x_{\text{zero}}(t)| = \frac{3}{2[1 + \epsilon \cos(t + \phi)]}$. This perturbed potential presents an oscillating minimum on $x_{\text{min}}(t) = -\frac{1}{1 + \epsilon \cos(t + \phi)}$, for which the value of this perturbed potential is $\Delta V_{\text{min}}(t) = -\frac{1}{6[1 + \epsilon \cos(t + \phi)]^2}$, so it oscillates around the unperturbed value $V(-1) = -1/6$.

III. NUMERICAL EVIDENCE TO AVOID ESCAPES USING PHASE CONTROL

In this section we provide numerical evidence showing that by using an adequate value of ϕ and ϵ , we can avoid escapes for this system. A first numerical evidence about the effect of the control in the system can be observed in Fig. 4. Figure 4(a) shows a typical escaping trajectory for $F=0.21$ with initial condition at $(x_0, \dot{x}_0) = (-0.5, -0.1)$, in the absence of control. If we introduce the control, say $\epsilon=0.05$, and a value of phase $\phi=\pi$ the particle does not escape from the well, as is observed in Fig. 4(b).

We have explored this phenomenon in detail numerically. To do this, we have performed a numerical integration of trajectories whose initial conditions belong to a 60×60 grid in the phase space region $x \in [-1.5, 0.5]$, $\dot{x} \in [-0.7, 0.7]$ for different combinations of ϵ and ϕ , and observed which of them escape. In the diagrams plotted in Figs. 5(a)–5(c) the rates of particles that do not escape as a function of ϵ and ϕ are shown. Note that in some regions of these diagrams, for

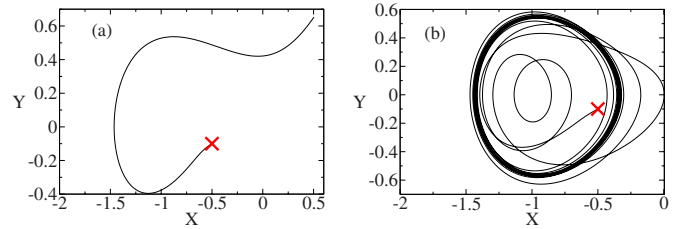


FIG. 4. (Color online) (a) Single trajectory for the Helmholtz oscillator $\ddot{x} + 0.1\dot{x} - x - x^2 = 0.21 \cos t$, with initial condition at the point $(x_0, \dot{x}_0) = (-0.5, -0.1)$ as indicated by the cross. The particle escapes after a lapse of time. (b) Single trajectory [as in Fig. 4(a)] for the Helmholtz oscillator with control, $\ddot{x} + 0.1\dot{x} - [1 + 0.05 \cos(t + \pi)]x^2 = 0.21 \cos t$. The perturbation keeps the particle in the well forever. (Notice that $y = \dot{x}$.)

example for $\epsilon \approx 0.1$ and $\phi = \pi$, more than 50% of the particles are kept bounded. This is quite surprising since a value of ϵ of this order has a very small effect on the shape of the well. However, if we take another value of the phase ϕ , such as $\phi = 0$, nearly all trajectories escape. Thus the role of the phase ϕ is crucial if we want to keep the trajectories bounded.

This modulation can be quantified as follows. Assuming that we set $\cos(t + \phi) = 1$, the depth of the well becomes $\Delta V = \frac{1}{6(1 + \epsilon)^2}$ and the width $\Delta x = \frac{3}{2(1 + \epsilon)}$. Note that the width of the potential (see Fig. 1) is the distance between the local maximum x_{max} and the point $x_{\text{min}} = -\frac{3}{2(1 + \epsilon)}$. The effect of the modulation in these quantities is summarized in Table I. We observe that by changing only a little bit the shape of the potential we can control escapes in some specific regions of phase space.

The typical basins of attraction of the Helmholtz oscillator after having applied the phase control for $F=0.21$, $\phi=\pi$ and modulation amplitudes $\epsilon=0.05$, $\epsilon=0.055$, $\epsilon=0.1$, and $\epsilon=0.15$, respectively, are plotted in Fig. 6. Observe the strong effects of this term ϵ and the phase ϕ on the basin of attraction of bounded orbits, whose area grows drastically with ϵ once we choose a suitable value of the phase $\phi=\pi$. This is due to the underlying phenomenon consisting in a bifurcation in the basins of attraction from fractal to nonfractal due to the strong effect of the attractor(s) when the modulation amplitude ϵ increases. As we show in Fig. 7(a) this phenomenon takes place for a value of $\epsilon = \epsilon_c \geq 0.05$ and this transition occurs between Fig. 6 (top left) and Fig. 6 (top right). This means that for the value ϵ_c a rapid decrease in the fractal dimension is expected and also an increase of the area of the basin of attraction [marked in cyan (pale gray)]. To explain this, notice that as ϵ increases, following the arguments that will be given in Sec. IV, the effect is analogous to have a deeper potential, so the system loses its unpredictability because most of the particles are trapped in the well [17]. This loss of unpredictability implies that the basin boundaries become smoother and therefore a decrease in the fractal dimension causes this bifurcation. Besides, this phenomenon occurs because the strong effect of the attractor(s) once ϵ is above its critical value ϵ_c . This produces a ratio of particles that falls as the attractor(s) increase(s) and therefore the area of the basin of attraction, as shown clearly in Fig. 6 (top right

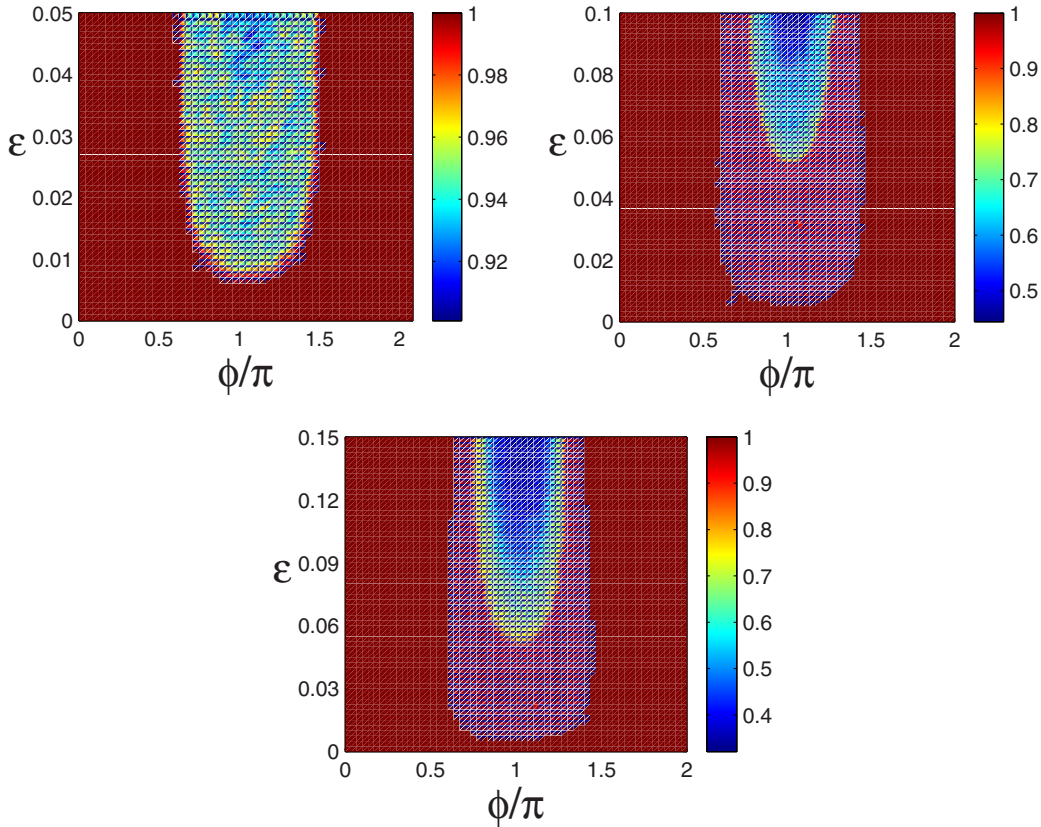


FIG. 5. (Color online) Color plot of the fraction of trajectories with initial conditions in the region $[-1.5, 0] \times [-0.7, 0.7]$ that escape to infinity for different values of ϵ and ϕ . Note that an adequate choice of the phase ϕ is critical if we are interested in avoiding escapes, and that apparently the optimal values of the phase for this purpose are located around $\phi = \pi$.

and top left). Considering this, we speculate that this phenomenon might be related with a basin boundary metamorphosis [18]. However, to elucidate this point, which might not be trivial due to the coexistence of more than two attractors, is out of the scope of the present work. From a purely control point of view, considering that our aim in this work is to prevent escapes of the trajectories, we want to emphasize that the important feature that these calculations reveal is that, for ϵ_c , there is a sudden increase in the area of the basins of attraction corresponding to bounded orbits. This is important in this context as long as it implies that the fraction of initial conditions that will not escape for this system also increases drastically for $\epsilon \approx \epsilon_c$. A similar phenomenon of the Helmholtz oscillator produced when we vary the dissipation parameter instead of the modulation amplitude is thoroughly studied in Ref. [19].

TABLE I. Variation of the width Δx and depth ΔV of the well as a function of ϵ . The percentages $\% \Delta x$ and $\% \Delta V$ indicate the percentage variation in the width and the depth of the potential well for the chosen values of ϵ .

ϵ	Δx	ΔV	$\% \Delta x$	$\% \Delta V$
0	1.50	0.16	0	0
0.05	1.43	0.15	4.5	9.5
0.10	1.36	0.14	8.8	15
0.15	1.31	0.13	11.6	21

In order to complete our numerical study we have estimated the escape times of the particles for different initial conditions fixing the modulation amplitude ϵ and the phase ϕ separately. Notice that a certain percentage of the particles never escapes, having infinite escape times. Since it is not possible to numerically compute most of the escape times, the times of integration have been bounded. For this purpose, we have stopped the integration times to 3×10^4 time units because it is large enough to suppose that the particles are kept forever inside the well and never escape from it. We have plotted in Figs. 7(a) and 7(b) the behavior of the average escape times T for 100 different initial conditions chosen in the region $x \in [-1.5, 0]$ and for $\dot{x} = 0$. In Fig. 7(a) we fixed the phase to $\phi = \pi$ increasing the value of ϵ from 0 to 0.1. Here, we can observe some fluctuations in the escape times for small values of ϵ that do not obey any scaling law between T and ϵ . This fact is due to the effects of the appearance and disappearance of different attractors in the system as shown in Fig. 6. Once the modulation amplitude ϵ reaches a critical value $\epsilon_c \approx 0.05$ [this is clearly shown in Fig. 7(a)], T has a steep increase limited by the integration time t_{\max} . This result is in agreement with the basin bifurcation phenomenon explained in the previous paragraph and shown in Figs. 6(a) and 6(b). On the other hand, we have tested that, as t_{\max} is set above 300 time units (by testing different integration times up to 3×10^4) the plot of T versus ϵ is unmodified. This means that for $\epsilon < \epsilon_c$, only a fraction of the initial conditions yields confined trajectories and the complementary

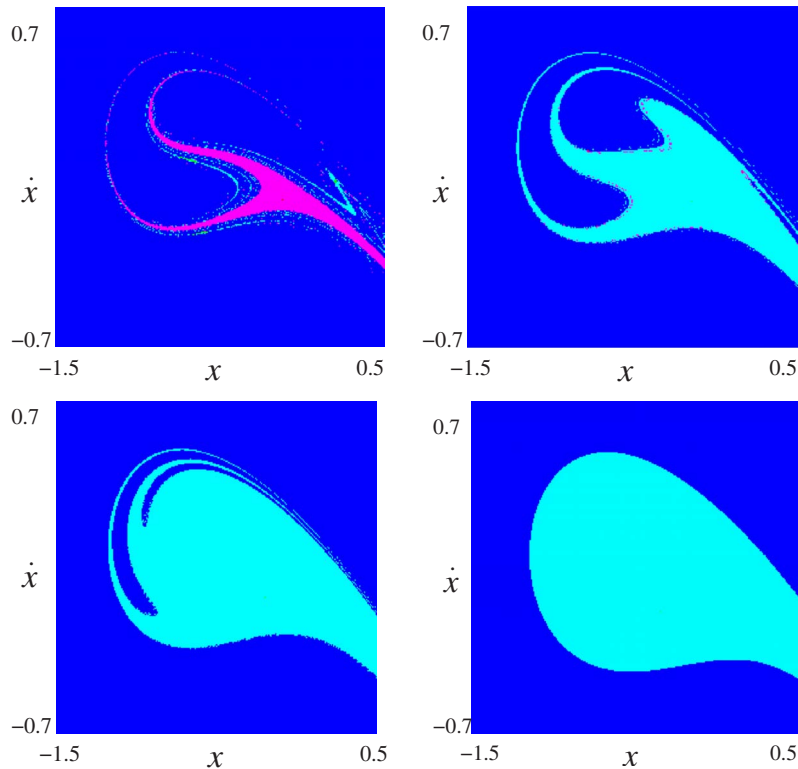


FIG. 6. (Color online) Basins of attraction of the perturbed Helmholtz oscillator $\ddot{x}+0.1\dot{x}-x-[1+\epsilon\cos(t+\pi)]x^2=0.21\cos t$, with modulation amplitudes $\epsilon=0.05$ (top left), $\epsilon=0.055$ (top right), $\epsilon=0.1$ (bottom left), and $\epsilon=0.15$ (bottom right), respectively. Blue (black) dots denote the points that escape from the potential well and cyan (pale gray) dots the points that fall into the attractor(s) [23].

fraction has escaped at various times less than t_{\max} . Thus, T results as a weighted sum, where the confined fraction enters with the value t_{\max} . Note that, in Fig. 7(a), for $\epsilon > \epsilon_c$, about 90% of the initial conditions yield confined trajectories and only 10% escape at times less than t_{\max} and, for $\epsilon < \epsilon_c$, the irregular T versus ϵ profile is due to the fractal structure of the basins, as shown in Fig. 6 (top left). Figure 7(b) shows, for $\epsilon=0.1$, the crucial role of the phase ϕ in the escape times

showing clearly that its optimal value takes place at $\phi_{\text{opt}} \approx \pi$, where the confined trajectories are clustered around the optimal value ϕ_{opt} . Finally, we have to indicate that the arguments given in the last two figures provide more numerical support and robustness to the results obtained during this section.

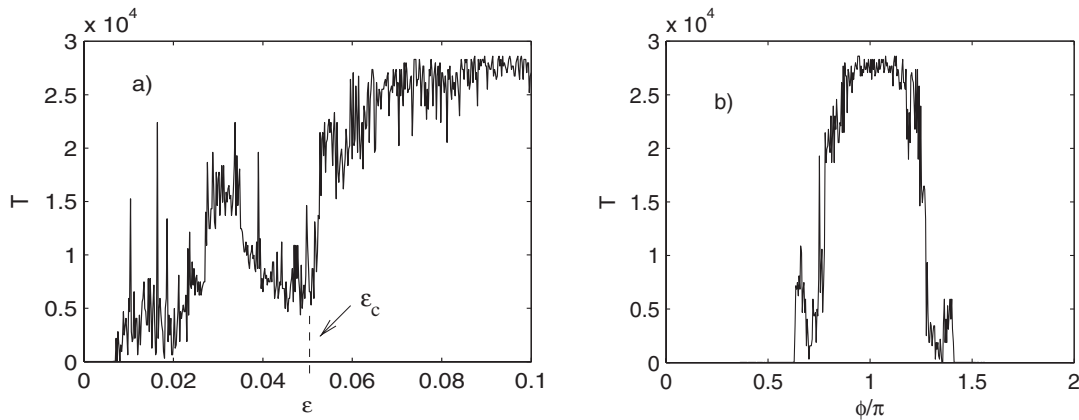


FIG. 7. (a) Plot of the average escape times T versus the modulation amplitude ϵ for a fixed value of the phase $\phi=\pi$ and 100 different initial conditions chosen in the region $x \in [-1.5, 0]$ and $\dot{x}=0$. In this figure we can observe some fluctuations of the average escape times for low values of ϵ and a rapid increasing to infinity (the integration time) for the escape times once that ϵ is large enough (above its critical value $\epsilon_c \approx 0.05$). (b) Plot of the average escape times T versus the phase ϕ for a fixed value of the modulation amplitude $\epsilon=0.1$ and 100 different initial conditions chosen in the region $x \in [-1.5, 0]$ and $\dot{x}=0$. The role of the phase is crucial to avoid escapes since in the region of values of phase $\phi \approx \pi$ the escape times are the highest.

IV. HEURISTIC ARGUMENTS FOR THE CONTROL OF ESCAPES

We have shown numerically that the harmonic modulation of the potential well with a suitable value of the phase ϕ are crucial to avoid escapes now. Now we provide a heuristic theory to explain the role of the phase ϕ in the control of escapes. We have seen that the effect of the perturbation in this system is analogous to applying a perturbation on the potential. In fact, the width of the perturbed potential well oscillates in time as $|\Delta x_{\text{zero}}(t)| = \frac{3}{2[1+\epsilon \cos(t+\phi)]}$, and the depth of this perturbed potential well also oscillates around the unperturbed value, according to the expression $\Delta V_{\text{min}}(t) = -\frac{1}{6[1+\epsilon \cos(t+\phi)]^2}$.

The maximum value of the forcing in the positive direction of the x axis corresponds to $t=0$, for which the value of the forcing is $F(t) = F_{\text{max}} \cos \omega t$, being $F = F_{\text{max}}$. For this value $F = F_{\text{max}}$, the deeper the potential well is, the more difficult is for the particles to escape. It takes place when $\phi = \pi$ for which the minimum of the potential reaches its minimum value and the depth of the potential is maximum, $|\Delta V| = \frac{1}{6(1-\epsilon)^2}$. Furthermore, for this situation, the width of the potential reaches its maximum value $|\Delta x_{\text{zero}}| = \frac{3}{2(1-\epsilon)}$ and it makes as a consequence the possibility to escape more difficult. Summarizing, these simple arguments in which $\phi = \pi$ show that the potential well reaches the maximum values of both, depth and width, becoming more difficult for the particles to escape from the well and even keeping them inside it and they can never escape.

Note that this heuristic argument agrees well with the optimal value of the phase found numerically. This idea is also confirmed by the experiments shown in next section, where this control method has been implemented in an electronic circuit that mimics the dynamics of our system.

V. EXPERIMENTAL EVIDENCE USING AN ELECTRONIC CIRCUIT

In this section our goal is to test our control technique in a laboratory system, and to confirm what we have observed numerically, i.e., that an adequate value of the phase difference ϕ between the main driving and the controlling perturbation can avoid escapes in the system. With this purpose we have designed and built the electronic circuit sketched in Fig. 8. This circuit mimics the dynamics of the Helmholtz oscillator. A similar circuit was used in Ref. [22]. Our circuit consists of an electronic analog simulator implemented using commercial semiconductor devices. V_d is the driving voltage amplitude, applied by the generator G_d , while V_c is the control voltage amplitude applied by means of an arbitrary function generator TABOR 8024. The two sinusoidal signals V_d and V_c have the same frequency and the value of the phase ϕ is fixed for $t=0$, so it is constant in the experiment. Thus, following the main idea of the phase control scheme, once the phase ϕ is chosen no further adjustment of its value needs to be done during the experiment. The integrators I_1 and I_2 have been implemented using Linear Technology LT1114CN four quadrant operational amplifiers, while the multipliers are Analog Devices MLT04. The acqui-

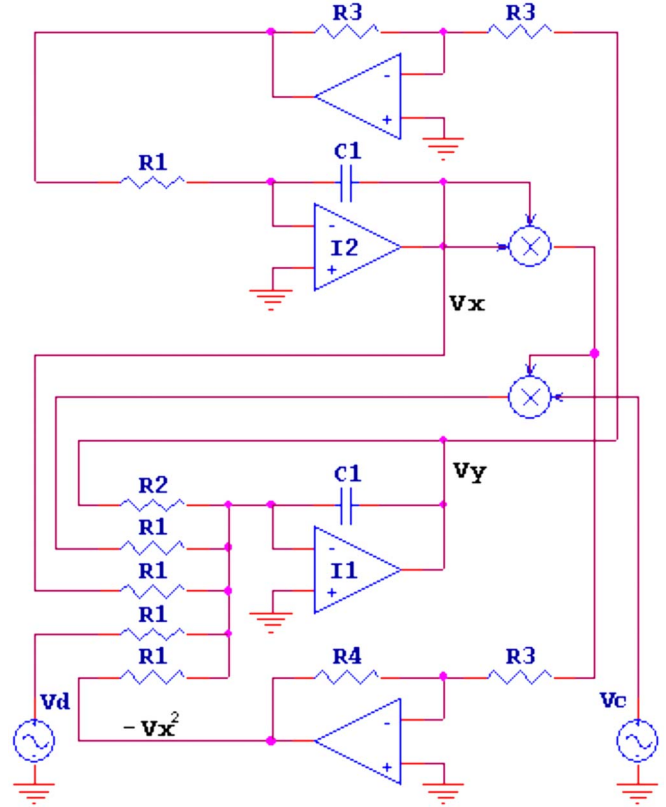


FIG. 8. (Color online) Layout of the electronic circuit. I : integrators; R : resistors; C : capacitors; X : multipliers; V_d : sinusoidal driving signal; V_c : sinusoidal control signal. Under a suitable time normalization, the dynamics is ruled by the equation $\ddot{x} + 0.1\dot{x} - x - [1 + \epsilon \cos(t + \phi)]x^2 = 0.21 \cos t$, where $x \propto V_x$ and $\dot{x} \propto V_y$. The parameters ϵ, ϕ are fixed by the arbitrary wave form generator V_c . The numerical values are $R_1 = 100 \text{ K}\Omega$, $R_2 = 1 \text{ M}\Omega$, $R_3 = 2 \text{ K}\Omega$, $R_4 = 5 \text{ K}\Omega$, and $C_1 = 10 \text{ nF}$.

sition of the experimental data has been performed by means of a TEKTRONIX TDS 7104 digital oscilloscope connected to a personal computer. Under suitable time scale normalization the dynamics of this circuit is governed by Eq. (5), where the parameters are $\delta = 0.1$, $F = 0.2$, and $\omega = 1$, and the amplitude of the applied control is $\epsilon \approx 0.03$. The voltages of the circuit V_x and V_y can be associated to x and \dot{x} , respectively.

Different trajectories in phase space observed experimentally, corresponding to different values of the main driving amplitude V_d , are shown in Fig. 9. The chaotic attractor that can be observed for sufficiently low values of V_d is shown in Fig. 9(a). A diverging trajectory can be seen in Fig. 9(b). Finally, a periodic orbit observed for smaller values of the driving amplitude V_d smaller than the one leading to chaotic motion is shown in Fig. 9(c).

In order to test the validity of the control technique, we have performed different bifurcation diagrams of the system for different values of the amplitude of the perturbation ϵ and for a fixed value of the phase ϕ . In these bifurcation diagrams we capture the dynamics of the system for different values of the amplitude of the main forcing V_d . These diagrams have been performed by slowly varying the value of

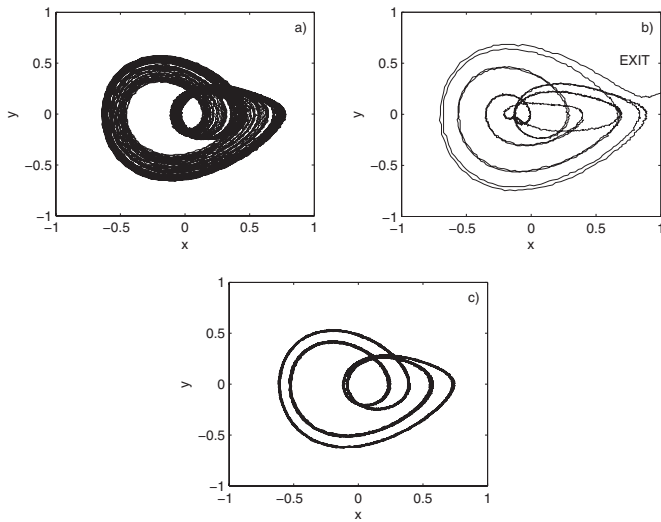


FIG. 9. Single trajectories in the experimental electronic circuit simulating the Helmholtz oscillator where we can find different dynamics. (a) Chaotic attractor. (b) Escaping trajectory. (c) Periodic orbit. (Notice that $y=\dot{x}$.)

the forcing and by reporting the maxima of the resulting long time series. This way we can see the behavior of the system for different values of the forcing amplitude. In Fig. 10(a) we can see the experimental bifurcation diagram in the absence of any external perturbations ($\epsilon=0$). This diagram clearly shows a transition to chaos through a period-doubling cascade, after which there is a boundary crisis by which the chaotic attractor disappears and the particles escape to the

infinity. The situation changes if we apply a perturbation with the suitable fixed value of the phase $\phi=\pi$. The resulting bifurcation diagram, which is shown in Fig. 10(b), shows that the boundary crisis and the divergence of the trajectories takes place for a value of the driving amplitude that is higher than in the unperturbed case. This implies that trajectories that would typically diverge to infinity are kept bounded for this value of ϕ .

Thus, our experiment confirms that an adequate choice of the phase ϕ becomes crucial as well in this experiment. In Fig. 10(c) we can see that with fixed value of the phase $\phi=0$ the attractor is destroyed for a value of the main driving V_d sensibly smaller than the one reported in the unperturbed case. Thus, we can see once more that the value of ϕ plays a key role in the global dynamics of the system.

From an experimental point of view, it is interesting to consider which would be the effect of a mismatch between the frequency of the main driving and the frequency of the controlling perturbation, a situation that may arise in some experimental implementations. Considering that mismatch, the controlling perturbation applied to the system can be written as $\epsilon \cos[(\omega + \delta\omega)t + \phi_{opt}]$, where $\delta\omega \ll 1$ would be the value of the frequency mismatch. This perturbation can be rewritten as $\epsilon \cos[\omega t + \phi(t)]$, where $\phi(t) \equiv \phi_{opt} + \delta\omega t$ is the new phase difference that slowly varies in time. However, as long as the phase $\phi(t)$ remains in the interval for which trajectories remain bounded (detected numerically in Sec. III) divergences are not expected, and the smaller $\delta\omega$ is the longer our phase control method will keep the trajectories bounded. Thus, in the presence of a frequency mismatch our scheme allows us to keep trajectories bounded for a period of

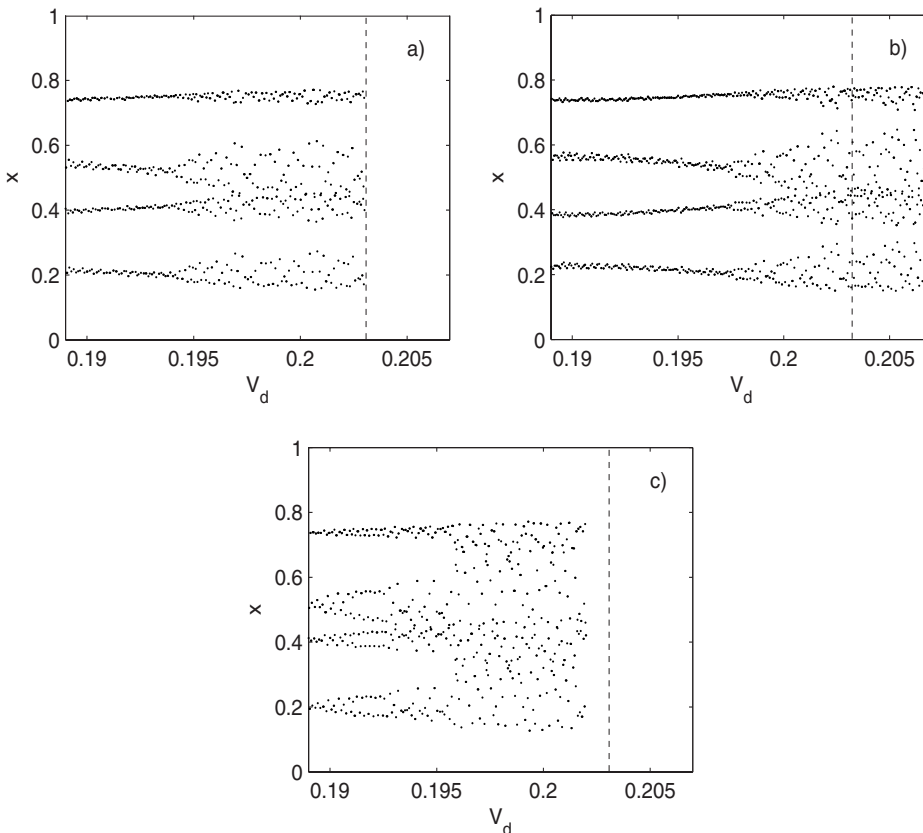


FIG. 10. Experimental bifurcation diagrams obtained from the circuit. These diagrams represent the variable x against the driving voltage V_d . We can observe different boundary crises: (a) without control, (b) for $\epsilon=0.05$ and $\phi=\pi$, (c) for $\epsilon=0.05$ and $\phi=0$. In every figure we can test that the modulation amplitude ϵ and an accurate value of the phase $\phi=\pi$ are fundamental for the control of escapes. Observe that in all figures dashed lines denote, in absence of control, the point in the bifurcation diagram in which the boundary crisis would take place.

time that scales as $1/\delta\omega$. This feature is shared by most control methods based on the application of a small harmonic perturbation to the system.

Finally, we want to emphasize that the implementation of our control scheme on an electronic circuit provides more evidence about its robustness. For example, we have to notice that imperfections in the circuit's multipliers imply that the potential that we obtain is not exactly a cubic potential like the one that we have analyzed numerically. On the other hand, environmental noise is present in the circuit, as in most realistic experimental situations. But, in spite of all this, we have observed that most of the important features of our control scheme that were observed numerically have been recovered in its implementation on the circuit. This makes us think that the phase control method is a versatile technique that can be applied to avoid escapes in a wide variety of situations.

VI. CONCLUSIONS AND DISCUSSION

In conclusion, by using as a prototype model the Helmholtz oscillator and the phase control technique, we have shown that an adequate parametric perturbation in the quadratic term of the equation of motion of this oscillator can avoid escapes in some regions in phase space. We provide numerical support and heuristic arguments for which we con-

trol the orbits in the well, avoiding the escapes from it by simply changing slightly the depth and width of the well and by using a suitable value of the phase ϕ . We have shown the robustness and the general nature of this method in the sense that the experimental implementation of a circuit confirms the same results. In the context of physical situations, the problems with escapes are typical in chaotic scattering problems, which have applications in many fields in physics. We expect this work to be useful for a better understanding of systems with escapes because our system is a paradigmatic one-dimensional system and the results can be, in principle, generalized for higher dimensional problems and any open dynamical system.

ACKNOWLEDGMENTS

We would like to thank Inés P. Mariño for the fruitful discussions we had during the development of this work. This work was supported by the Spanish Ministry of Science and Technology under Project No. BFM2003-03081, by the Spanish Ministry of Education and Science under Project No. FIS2006-08525, and by Universidad Rey Juan Carlos and Comunidad de Madrid under Projects No. URJC-CM-2006-CET-0643 and No. URJC-CM-2007-CET-1601. J.S. and S.Z. acknowledge the warm hospitality received at Istituto Nazionale di Ottica Applicata where part of this work was carried out.

-
- [1] T. Tel, in *Directions in Chaos*, edited by H. Bai-Lin (World Scientific, Singapore, 1990), pp. 149–211.
 - [2] Some representative early papers on chaotic scattering are C. Jung, *J. Phys. A* **19**, 1345 (1986); M. Hénon, *Physica D* **33**, 132 (1988); P. Gaspard and S. A. Rice, *J. Chem. Phys.* **90**, 2225 (1989); G. Troll and U. Smilansky, *Physica D* **35**, 34 (1989).
 - [3] M. Ding, C. Grebogi, E. Ott, and J. A. Yorke, *Phys. Rev. A* **42**, 7025 (1990).
 - [4] For a relatively early review of chaotic scattering, see: *Chaos* **3** (4) (1993), Focus Issue.
 - [5] S. Bleher, C. Grebogi, and E. Ott, *Physica D* **46**, 87 (1990).
 - [6] G. Contopoulos and M. Harsoula, *Ann. N. Y. Acad. Sci.* **1045**, 139 (2005).
 - [7] E. Ott, C. Grebogi, and J. A. Yorke, *Phys. Rev. Lett.* **64**, 1196 (1990).
 - [8] J. Aguirre, F. d'Ovidio, and M. A. F. Sanjuán, *Phys. Rev. E* **69**, 016203 (2004).
 - [9] S. Boccaletti, C. Grebogi, Y. C. Lai, H. Mancini, and D. Maza, *Phys. Rep.* **329**, 103 (2000).
 - [10] R. Lima and M. Pettini, *Phys. Rev. A* **41**, 726 (1990).
 - [11] R. Meucci, W. Gadamski, M. Ciofini, and F. T. Arecchi, *Phys. Rev. E* **49**, R2528 (1994).
 - [12] Z. Qu, G. Hu, G. Yang, and G. Qin, *Phys. Rev. Lett.* **74**, 1736 (1995).
 - [13] S. Zambrano, E. Allaria, S. Brugioni, I. Leyva, R. Meucci, M. A. F. Sanjuán, and F. Arecchi, *Chaos* **16**, 013111 (2006).
 - [14] S. Zambrano, I. P. Mariño, F. Salvadori, R. Meucci, M. A. F. Sanjuán, and F. T. Arecchi, *Phys. Rev. E* **74**, 016202 (2006).
 - [15] J. Lehmann, P. Reimann, and P. Hänggi, *Phys. Rev. Lett.* **84**, 1639 (2000).
 - [16] J. M. Casado and M. Morillo, *Phys. Rev. E* **49**, 1136 (1994).
 - [17] J. M. Seoane, M. A. F. Sanjuán, and Y. C. Lai, *Phys. Rev. E* **76**, 016208 (2007).
 - [18] C. Grebogi, E. Ott, and J. A. Yorke, *Phys. Rev. Lett.* **56**, 1011 (1986).
 - [19] J. A. Almendral, J. M. Seoane, and M. A. F. Sanjuán, *Recent Res. Dev. Sound Vib.* **2**, 115 (2004).
 - [20] J. A. Almendral and M. A. F. Sanjuán, *J. Phys. A* **36**, 695 (2003).
 - [21] H. Cao, J. M. Seoane, and M. A. F. Sanjuán, *Chaos, Solitons Fractals* **34**, 197 (2007).
 - [22] E. del Río, A. Rodríguez Lozano, and M. G. Velarde, *Rev. Sci. Instrum.* **63**, 4208 (1992).
 - [23] The basins of attraction (Figs. 2 and 6) have been computed using the software DYNAMICS: H. E. Nusse and J. A. Yorke, *Dynamics: Numerical Explorations* (Springer, New York, 1997).